

## Observing Information Backflow from Controllable Non-Markovian Multichannels in Diamond

Ya-Nan Lu<sup>1,2,\*</sup>, Yu-Ran Zhang,<sup>3,\*</sup> Gang-Qin Liu<sup>1,4,†</sup>, Franco Nori<sup>3,5</sup>, Heng Fan,<sup>1,4,6,‡</sup> and Xin-Yu Pan<sup>1,4,6,§</sup>

<sup>1</sup>*Institute of Physics, Chinese Academy of Sciences, Beijing 100190, China*

<sup>2</sup>*School of Physical Sciences, University of Chinese Academy of Sciences, Beijing 100049, China*

<sup>3</sup>*Theoretical Quantum Physics Laboratory, RIKEN Cluster for Pioneering Research, Wako-shi, Saitama 351-0198, Japan*

<sup>4</sup>*Songshan Lake Materials Laboratory, Dongguan, Guangdong 523808, China*

<sup>5</sup>*Physics Department, University of Michigan, Ann Arbor, Michigan 48109-1040, USA*

<sup>6</sup>*CAS Center of Excellence in Topological Quantum Computation, Beijing 100190, China*



(Received 4 January 2020; accepted 20 April 2020; published 27 May 2020)

The unavoidable interaction of a quantum open system with its environment leads to the dissipation of quantum coherence and correlations, making its dynamical behavior a key role in many quantum technologies. In this Letter, we demonstrate the engineering of multiple dissipative channels by controlling the adjacent nuclear spins of a nitrogen-vacancy center in diamond. With a controllable non-Markovian dynamics of this open system, we observe that the quantum Fisher information flows to and from the environment using different noisy channels. Our work contributes to the developments of both noisy quantum metrology and quantum open systems from the viewpoints of metrologically useful entanglement.

DOI: [10.1103/PhysRevLett.124.210502](https://doi.org/10.1103/PhysRevLett.124.210502)

Any realistic quantum system is inevitably subject to an external environment. This environment makes the open-system dynamics significant for many quantum technologies, such as entangled-state engineering [1–3], quantum simulation [4], and quantum sensing [5]. The ordinary environment, usually consisting of a large number of degrees of freedom, is hard to control, despite some attempts on controllable transitions from Markovian to non-Markovian dynamics [6–11]. A Markovian process assumes memoryless dynamics of a quantum open system, with the information continuously flowing to its environment, which is described by a dynamical semigroup with a time-independent Lindblad generator [12]. However, in the presence of memory effects, e.g., for a strong system-environment coupling, the Markovian approximation fails, and the non-Markovian process, deviating from the dynamical semigroup, allows for a revival of quantum features, via the backflow information from the environment. Therefore, whether the open-system dynamics is Markovian or non-Markovian can be characterized by the orientation of the information flow between the system and the environment [13].

Owing to the memory effects and the ability of recovering quantum features, non-Markovian quantum dynamics [14,15] opens a new perspective for applications in quantum metrology. Quantum metrology [16,17], an emerging quantum technology, aims to use quantum resources to yield a higher precision of statistical errors in estimating parameters compared to classical approaches. Quantum metrological studies can be very different when being subject to either Markovian or non-Markovian noises [18]. In addition, the metrologically useful quantum

coherence and multipartite entanglement are essentially quantified by the quantum Fisher information (QFI) [19,20]. Thus, it is important to establish an approach for characterizing the non-Markovianity of the open-system dynamics by using the QFI flow between the quantum system and its environment [21]. Other measures of non-Markovianity include bipartite entanglement [22–24], trace distance [25], and temporal steering [26]. As a comparison, the metrological approach based on QFI also works on the information subflows through different dissipative channels for a class of time-local master equations [21].

In this Letter, we engineer multiple dissipative channels of an open system and use QFI to quantify its non-Markovian dynamics. The backflow of QFI, as a witness of the non-Markovian dynamics, is observed in both the quantum coherence and two-qubit entanglement experiments. Our results also show that QFI flow can be decomposed into additive subflows according to different dissipative channels.

In our experiments, the open system is provided by a nitrogen-vacancy (NV) center electron spin, its host <sup>14</sup>N nuclear spin, and a proximal <sup>13</sup>C nuclear spin in diamond (see Fig. 1). Details of the sample are presented in Supplemental Material [27], which includes Refs. [28–38]. Applying the secular approximation and ignoring the weak nuclear-nuclear dipolar interactions, the effective interaction Hamiltonian of the three-qubit system and the spin bath can be written as [39] (we set  $\hbar = 1$ )

$$\hat{\mathcal{H}}_I = A_n^{\parallel} \hat{S}_e^z \hat{I}_n^z + A_c^{\parallel} \hat{S}_e^z \hat{I}_c^z + \hat{H}_R, \quad (1)$$

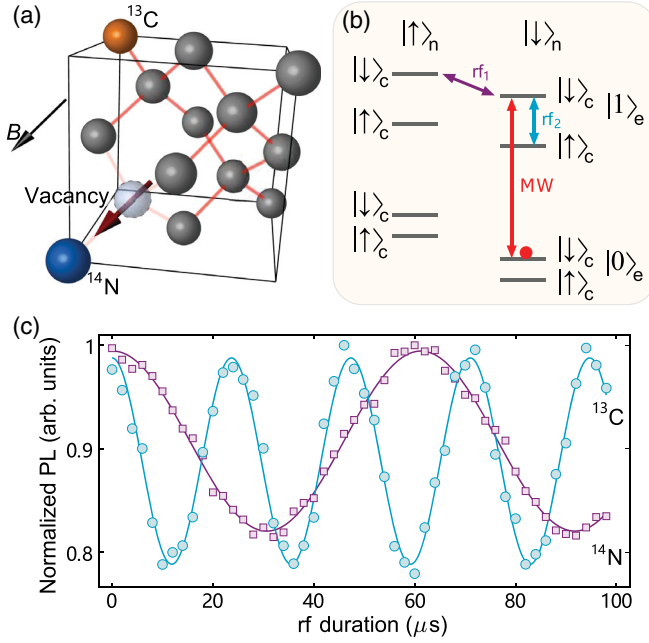


FIG. 1. Coherent manipulation of multiple spins in diamond. (a) The nitrogen-vacancy (NV) center, its host  $^{14}\text{N}$  nuclear spin, and a nearby  $^{13}\text{C}$  nuclear spin form a three-qubit system. (b) Energy levels of the three-qubit system. At the excited-state level anticrossing (ESLAC), the three spin qubits can be polarized by a short laser pulse and manipulated with resonant radio-frequency (rf) pulses (13.284 MHz for the  $^{13}\text{C}$  nuclear spin and 2.929 MHz for the host  $^{14}\text{N}$  nuclear spin). (c) Rabi oscillations of the  $^{14}\text{N}$  and  $^{13}\text{C}$  nuclear spins under an external magnetic field of  $B = 482$  G along the quantization axis of the NV center (NV electron spin is at the  $m_s = -1$  state).

where  $\hat{H}_R$  is the interaction Hamiltonian between the electron qubit and the spin bath,  $A_n^{\parallel} \simeq -2.16$  and  $A_c^{\parallel} \simeq 12.8$  MHz denote the hyperfine coupling strengths between the electron spin and nearby nuclear spins, respectively.

Under an external magnetic field of  $B_z = 482$  G, the electron spin and nearby nuclear spins can be simultaneously polarized by a short laser pump due to level anticrossing in the excited state (ESLAC) [40]. In Fig. 1(c), we show Rabi oscillations of the  $^{13}\text{C}$  and  $^{14}\text{N}$  nuclear spins, driven by 13.284 and 2.929 MHz radio-frequency (rf) pulses, respectively. The dephasing time  $T_{2n}^*$  of the host  $^{14}\text{N}$  nuclear spin is about 5.5 ms, limited by the spin relaxation of the NV electron spin ( $T_{1e} = 6.4 \pm 0.4$  ms). A shorter dephasing time  $T_{2c}^*$  (about 0.6 ms) of the  $^{13}\text{C}$  nuclear spin is observed, which may be caused by the 3 times larger gyromagnetic ratio of  $^{13}\text{C}$  and its coupling to other nuclear spins. The nearby nuclear spins form a natural non-Markovian environment with a long coherence time [41]. However, in our experiments, we focus on the dephasing process (free induction decay, FID) of the electron spin ( $T_{2e}^* = 2.9 \pm 0.1$   $\mu\text{s}$ ). During the hours of FID measurements, all the possible configurations of the nuclear spin bath have been averaged out, resulting in a Markovian decay of information [9].

In the first experiment, we employ the electron qubit as a noise sensor, whose dynamical behavior is modulated by initializing the state of the host  $^{14}\text{N}$  spin and the proximal  $^{13}\text{C}$  spin [see Fig. 2(a)]. Since the interactions between nuclear spins can be ignored in the timescale of our experiments, these two controllable nuclear spins can be regarded as the regulators of two independent dissipative channels, and other weakly coupled nuclear spins act as another uncontrollable dissipative channel (see Supplemental Material [27] for details). The quantum circuits and pulse sequences of the first experiment are shown in Figs. 2(c) and 2(e), respectively. By applying a 3- $\mu\text{s}$  laser pulse (532 nm), these three qubits are polarized to an initial state  $|\Psi_i\rangle = |0\rangle_e \otimes |\downarrow\rangle_n \otimes |\downarrow\rangle_c$  (each subscript corresponds to its physical carrier). Then, by applying the microwave (MW),  $rf_1$  and  $rf_2$  pulses as shown in Fig. 2(e), the system is prepared in  $|\Psi(0)\rangle = |+\rangle_e \otimes |\psi(\phi_1)\rangle_n \otimes |\psi(\phi_2)\rangle_c$ , where  $|+\rangle_e \equiv (|0\rangle_e + |1\rangle_e)/\sqrt{2}$ , and  $|\psi(\phi)\rangle_{n,c} \equiv \cos(\phi/2)|\uparrow\rangle_{n,c} + \sin(\phi/2)|\downarrow\rangle_{n,c}$ , with  $\phi$  denoting the rf pulse duration. The time evolution of the electron qubit can be described by the partial trace after the unitary time evolution of the total Hamiltonian  $\hat{U}(t) = \exp(-i\hat{H}t)$  as  $\rho_e(t) = \text{Tr}_{\text{ncR}}[\hat{U}(t)\rho_0\hat{U}^\dagger(t)]$ , where  $\text{Tr}_{\text{ncR}}[\cdot]$  denotes the partial trace over the host  $^{14}\text{N}$  qubit, the  $^{13}\text{C}$  qubit and the spin bath degrees of freedom. Given the generator  $\hat{S}_e^z = \hat{\sigma}_e^z/2$ , the QFI of the electron qubit can be written as

$$\mathcal{Q}(t; \phi_1, \phi_2) = r^2(t) - s_z^2(t) \simeq \mathcal{Q}_n(t; \phi_1)\mathcal{Q}_c(t; \phi_2)\mathcal{Q}_R(t), \quad (2)$$

where  $r \equiv (s_x^2 + s_y^2 + s_z^2)^{1/2}$  is the length of the Bloch vector  $\mathbf{r} = [s_x, s_y, s_z]$ ;  $\mathcal{Q}_n(t) = 1 - \sin^2\phi_1 \sin^2(A_n^{\parallel}t/2 + \phi_1/2)$ ,  $\mathcal{Q}_c(t) = 1 - \sin^2\phi_2 \sin^2(A_c^{\parallel}t/2 + \phi_2/2)$ , and  $\mathcal{Q}_R(t)$  are the QFI of the electron qubit only subject to the  $^{14}\text{N}$ ,  $^{13}\text{C}$ , and the spin bath dissipative channels, respectively. The phase factors  $\phi_1$  and  $\phi_2$  represent the deviation of the prepared electron spin initial state from an ideal one. Details on  $\mathcal{Q}_R(t)$  and the phases can be found in the Supplemental Material [27].

The QFI flow, defined as the rate of change of the QFI,  $\mathcal{I}(t) \equiv \partial_t \mathcal{Q}(t; \phi_1, \phi_2)$ , can be explicitly written as a sum of QFI subflows with respect to different dissipative channels [21]

$$\mathcal{I}(t) = \mathcal{I}_n(t) + \mathcal{I}_c(t) + \mathcal{I}_R(t), \quad (3)$$

where  $\mathcal{I}_i(t) \equiv \mathcal{Q}(\partial_t \ln \mathcal{Q}_i)$ , with  $i = n, c, R$ , and each QFI subflow corresponds to not only the individual separable dissipative channel but also all channels [21]. Moreover, the inward QFI subflow ( $\mathcal{I}_i > 0$ ), resulting from the temporary appearance of a negative decay rate [31] of the time-local Lindblad master equation [12], is an essential feature of non-Markovian behaviors. Furthermore, we focus on the sum of time integrals of all inward QFI subflows

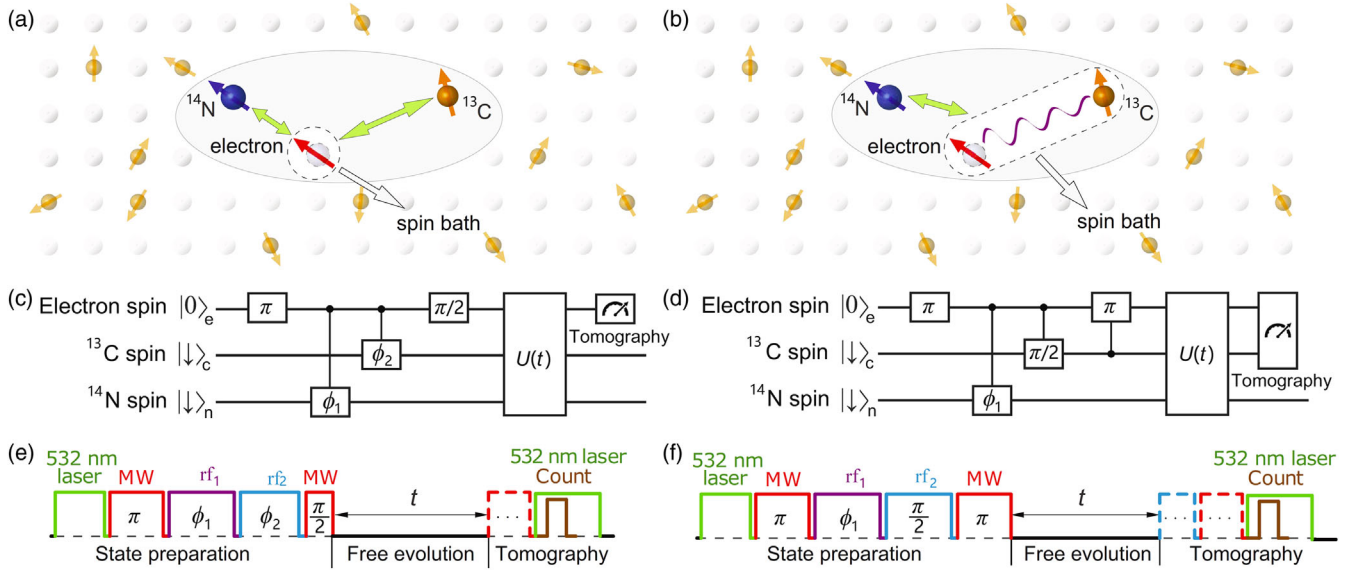


FIG. 2. Physical coding and experimental procedures. The NV electron spin and two strongly coupled nuclear spins play the roles of the open system and controlled dissipative channels, respectively, while the other (weakly coupled) nuclear spins form an uncontrolled dissipative channel. The quantum Fisher information (QFI) is used to characterize the quantum coherence and metrologically useful entanglement of the open system. (a) In the first experiment, the NV electron spin is the open quantum system. The quantum coherence of the system is subject to two controllable dissipative channels formed by the  $^{14}\text{N}$  and  $^{13}\text{C}$  nuclear spins. (b) In the second experiment, the electron spin and the  $^{13}\text{C}$  nuclear spin form the open system, and the entanglement between the two spins is subject to a controllable dissipative channel formed by the  $^{14}\text{N}$  nuclear spin. (c),(d) Quantum circuits and (e),(f) pulse sequences for the experiments. (The controlled gates are implemented by single-spin rotations in the corresponding subspaces.)

$$N(t, \phi_1, \phi_2) \equiv \sum_{i=n,c,R} \int_0^t dt \frac{|\mathcal{I}_i(\tau)| + \mathcal{I}_i(\tau)}{2}, \quad (4)$$

as a measure of non-Markovianity, and the long-time measure is defined as  $\mathcal{N}(\phi_1, \phi_2) \equiv N(t \rightarrow \infty, \phi_1, \phi_2)$ . Different from the time integral of the total QFI flow, the measure of non-Markovianity in Eq. (4) considers the inward subflow from each dissipative channel and can dig out the non-Markovianity even when the total QFI flow is negative.

In our experiments, the dissipative channels of the  $^{14}\text{N}$  and  $^{13}\text{C}$  qubits can be fully controlled by tuning the durations of the  $\text{rf}_1$  and  $\text{rf}_2$  pulses, i.e., to adjust  $\phi_1$  and  $\phi_2$ . When both channels are turned off,  $\phi_1 = \phi_2 = 0$  [see Fig. 3(a1) for the QFI], the dynamics of the NV electron spin is only affected by other weakly coupled  $^{13}\text{C}$  nuclear spins in the spin bath, and the QFI continuously flows out within the evolution time  $t \leq 600$  ns [see Fig. 3(a2)]. For  $\phi_1 = \pi/4, \pi/2$ , and  $\phi_2 = 0$ , the channel of the  $^{14}\text{N}$  nuclear spin is open, and the revival of the QFI is shown in Fig. 3(a1), while the positive QFI flows are observed in Figs. 3(a3) and 3(a4) for non-Markovian dynamics. For  $\phi_1 = 0$ , and  $\phi_2 = \pi/4, \pi/2$ , the revival of the QFI and the positive QFI flows, subject to the channels of the  $^{13}\text{C}$  nuclear spin and the spin bath, are plotted in Figs. 3(b1), 3(b2), and 3(b3). For fifteen experimental instances of  $^{13}\text{C}$  qubit's parameter  $\phi_2$ , the measured  $\mathcal{N}(0, \phi_2)$  is compared

with the numerical simulation (Fig. S5 in the Supplemental Material [27]).

We furthermore characterize the system behavior when both controllable dissipative channels are open. With  $\phi_1 = \phi_2 = \pi/2$ , the time evolution of the QFI of the electron qubit and its QFI flow, compared with the ones obtained from the sum of subflows (red cross), are shown in Figs. 3(c1) and 3(c2). In Fig. 3(c3), the measure of non-Markovianity  $\mathcal{N}[t, (\pi/2), (\pi/2)]$  from the QFI subflows,  $\mathcal{I}_{n,c,R}$ , with respect to different dissipative channels (red bar) is compared with the one from the total QFI flow,  $\mathcal{I}$  (blue bar). We clearly observe that the measure in terms of QFI subflows quantify more non-Markovianity than the total QFI flow, when the system is subject to multiple dissipative channels.

In the second experiment, we consider the open system, consisting of the electron qubit and the proximal  $^{13}\text{C}$  qubit, which is subject to the controllable noisy channel of the host  $^{14}\text{N}$  qubit and the dissipative channel of the spin bath [see Fig. 2(b)]. Figures 2(d) and 2(f) show the quantum circuit and pulse sequences of the second experiment. Starting with the state  $|\Psi_i\rangle = |0\rangle_e \otimes |\downarrow\rangle_n \otimes |\downarrow\rangle_c$ , the system is prepared in  $|\Psi'(0)\rangle = (|0\rangle_e \otimes |\downarrow\rangle_c + |1\rangle_e \otimes |\uparrow\rangle_c) \otimes |\psi(\phi_1)\rangle_n$ , with the pulse sequences shown in Figs. 2(d) and 2(f). The electron qubit and  $^{13}\text{C}$  nuclear qubit are maximally entangled at this stage. Similarly, assuming  $\rho'_0 = |\Psi'(0)\rangle\langle\Psi'(0)| \otimes \rho_R$ , the time evolution of the electron qubit and the  $^{13}\text{C}$  qubit is described as

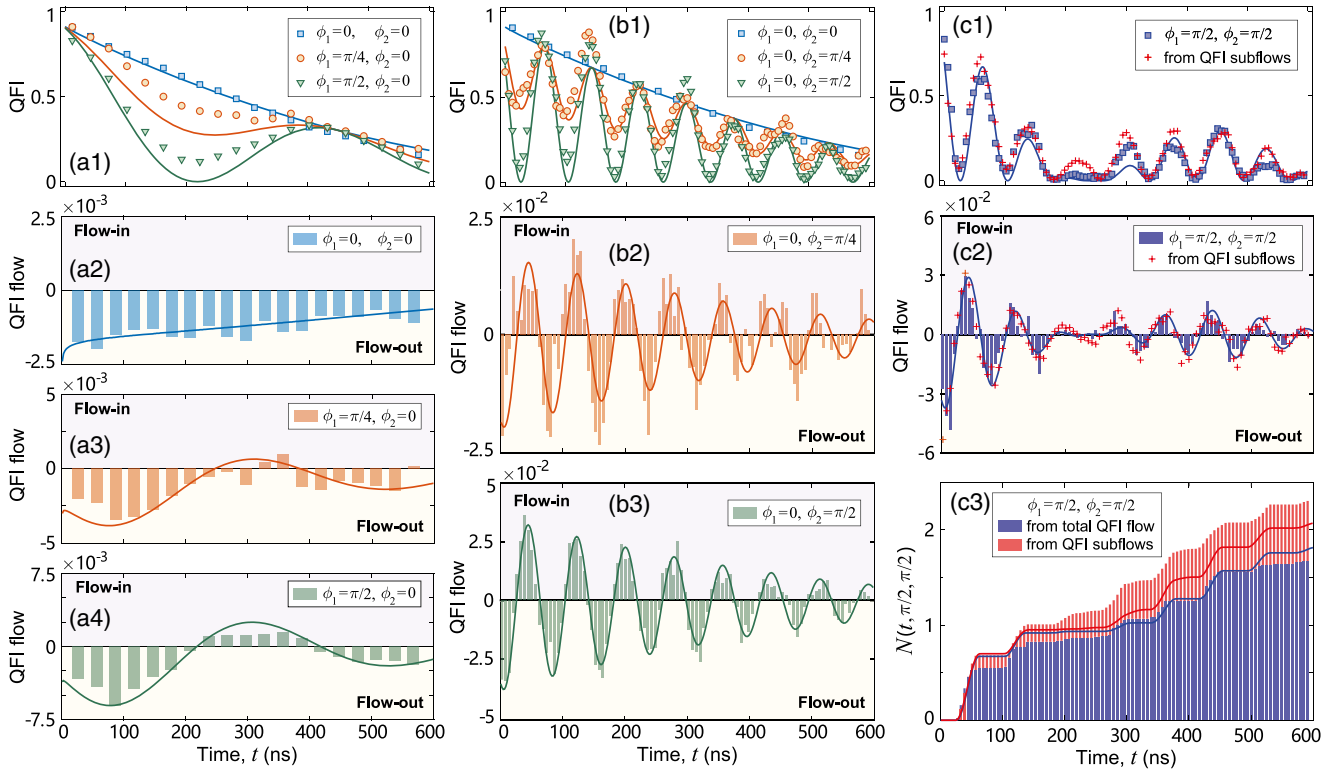


FIG. 3. QFI flows of the electron qubit in a controllable non-Markovian environment. Time evolution of the QFI with (a1) the dissipative channel of  $^{14}\text{N}$  open ( $\phi_1 = \pi/4, \pi/2$ ) and the one of  $^{13}\text{C}$  closed ( $\phi_2 = 0$ ); (b1) the dissipative channel of  $^{14}\text{N}$  closed ( $\phi_1 = 0$ ) and the one of  $^{13}\text{C}$  open ( $\phi_2 = \pi/4, \pi/2$ ); (c1) the dissipative channels of both nuclear spins open ( $\phi_1 = \phi_2 = \pi/2$ ) compared with the one calculated using the results of single channels given in (a1),(b1). QFI flows for the controllable dissipative channels with parameters: (a2)  $\phi_1 = \phi_2 = 0$ ; (a3)  $\phi_1 = \pi/4, \phi_2 = 0$ ; (a4)  $\phi_1 = \pi/2, \phi_2 = 0$ ; (b2)  $\phi_1 = 0, \phi_2 = \pi/4$ ; (b3)  $\phi_1 = 0, \phi_2 = \pi/2$ . (c2) When both dissipative channels are open, the total QFI flow is compared with the sum of subflows calculated by results in (a2),(a4),(b3). (c3) The measure of non-Markovianity from the total positive QFI flow in (c2) compared with the measure from the QFI subflows with respect to different dissipative channels  $[N[t, (\pi/2), (\pi/2)]]$  in Eq. (4), versus the evolution time. The solid curves are for the numerical simulations using experimental parameters.

$\rho'_{ec}(t) = \text{Tr}_{\text{nR}}[\hat{U}(t)\rho'_0\hat{U}^\dagger(t)]$ , where  $\text{Tr}_{\text{nR}}[\cdot]$  denotes the partial trace over the  $^{14}\text{N}$  spin and the spin bath degrees of freedom. If the QFI of a two-qubit state, with  $(\hat{S}_e^z + \hat{S}_c^z)$  being the generator, is larger than 2, i.e.,  $\mathcal{Q}'(t; \phi_1) > 2$ , it characterizes the useful entanglement for quantum-enhanced parameter estimation [16].

The time evolution of the QFI of the maximally entangled state is shown in Fig. 4(a), when the controllable  $^{14}\text{N}$  channel is either closed ( $\phi_1 = 0$ ) or open ( $\phi_1 = \pi/2$ ). At time  $t = 0$  with  $\phi_1 = 0$ , we obtain the maximum QFI,  $\mathcal{Q}'(0; 0) = 3.687$ , which is useful for sub-shot-noise-limit metrology [16,42]. With the dissipative channel of  $^{14}\text{N}$  closed ( $\phi_1 = 0$ ), the QFI flow remains negative [see Fig. 4(b)]. In Fig. 4(c), the positive QFI flow of the maximally entangled state, with  $\phi_1 = \pi/2$ , clearly signals the non-Markovian dynamics of the two-qubit open system. Moreover, the metrologically useful entanglement [ $\mathcal{Q}'(t; \phi_1) > 2$ ] survives for a period of time ( $\lesssim 380$  ns), when the open system only interacts with the weakly coupled  $^{13}\text{C}$  nuclear spins in the spin bath. However, it decays faster under the impact of non-Markovian noise by setting  $\phi_1 = \pi/2$ .

In summary, our experiments clearly demonstrate the control of the non-Markovian dynamics of open systems by manipulating the electron spin, the host  $^{14}\text{N}$ , and the neighboring  $^{13}\text{C}$  nuclear spins of the NV center in diamond at room temperature. First, the electron qubit, as an open system, is subject to two controllable dissipative channels of nearby nuclear qubits, of which the QFI flow characterizes the non-Markovianity and can be decomposed into subflows from individual channels. Second, when the open system, consisting of the electron qubit and the  $^{13}\text{C}$  qubit, is prepared in the maximally entangled state, the controllable non-Markovian behavior of the decoherence dynamics of the entanglement witnessed by the QFI flow is reported. By using the QFI as a witness for quantum coherence and metrologically useful entanglement, our work will contribute to the developments of both noisy quantum metrology [16,18,43] and the non-Markovian dynamics of quantum open systems in solids [42]. In addition, it will be helpful to investigate how our results can benefit applications of non-Markovianity [44–46], e.g., quantum computation [47] and quantum communication [48], by considering the anomalous decay effect in a spin bath [49,50].

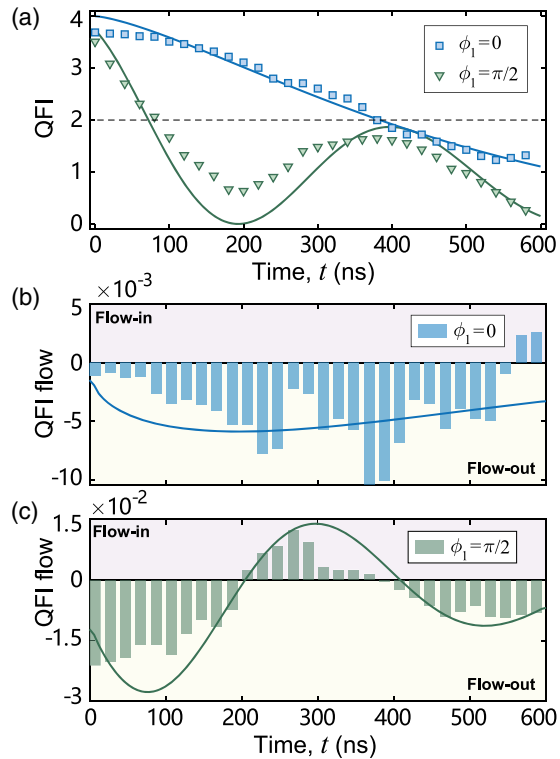


FIG. 4. (a) Time evolutions of the QFI of the maximally entangled state of the NV electron qubit and the 12.8 MHz  $^{13}\text{C}$  qubit with the controllable dissipative channel of the  $^{14}\text{N}$  qubit. QFI flows of the maximally entangled state with the controllable dissipative channel of  $^{14}\text{N}$  (b) closed ( $\phi_1 = 0$ ) and (c) open ( $\phi_1 = \pi/2$ ). The solid curves are for the numerical simulations using experimental parameters.

Although our experiments are carried out with an environment consisting of controllable dissipative channels, the verified relation between QFI and non-Markovianity is independent of the controllability of the environment [21]. Therefore, detecting the QFI of an open system is also helpful for quantitatively characterizing the non-Markovianity of the open-system dynamics in systems without the controllability of their environments, including but not limited to nuclear magnetic resonance [51], optical systems [7,11], superconducting qubits [52], and trapped ions [9]. Moreover, it is shown that with well-established control techniques of spins, the NV system is a powerful platform for studying complex open systems with multiple dissipative channels and developing possible applications of the memory effects in a non-Markovian dynamics.

We would like to acknowledge Zi-Yong Ge and Qing Ai for helpful discussions, and Da-Wei Lu for the codes of maximum likelihood estimation. This work was supported by the National Key Research and Development Program of China (Grants No. 2019YFA0308100, No. 2016YFA0302104, No. 2016YFA0300600), Strategic Priority Research Program of Chinese Academy of Sciences (Grant No. XDB28000000), and

NSFC (Grants No. 11974020, No. 11934018, No. 11574386). Y.R.Z. was supported by the China Postdoctoral Science Foundation (Grant No. 2018M640055) and the Japan Society for the Promotion of Science (JSPS) Postdoctoral Fellowship (Grant No. P19326). F.N. was supported in part by NTT Research, the Army Research Office (ARO) (Grant No. W911NF-18-1-0358), the Japan Science and Technology Agency (JST) (via the CREST Grant No. JPMJCR1676), the Japan Society for the Promotion of Science (JSPS) (JSPS-RFBR Grant No. 17-52-50023), and the Grant No. FQXi-IAF19-06 from the Foundational Questions Institute Fund (FQXi).

\*These authors contributed equally to this work.

†gqliu@iphy.ac.cn

‡hfan@iphy.ac.cn

§xypan@aphy.iphy.ac.cn

- [1] C. E. Bradley, J. Randall, M. H. Abobeih, R. C. Berrevoets, M. J. Degen, M. A. Bakker, M. Markham, D. J. Twitchen, and T. H. Taminiau, A Ten-Qubit Solid-State Spin Register with Quantum Memory Up to One Minute, *Phys. Rev. X* **9**, 031045 (2019).
- [2] A. Omran, H. Levine, A. Keesling, G. Semeghini, T. T. Wang, S. Ebadi, H. Bernien, A. S. Zibrov, H. Pichler, S. Choi, J. Cui, M. Rossignolo, P. Rembold, S. Montangero, T. Calarco, M. Endres, M. Greiner, V. Vuletić, and M. D. Lukin, Generation and manipulation of Schrödinger cat states in Rydberg atom arrays, *Science* **365**, 570 (2019).
- [3] C. Song, K. Xu, H. Li, Y.-R. Zhang, X. Zhang, W. Liu, Q. Guo, Z. Wang, W. Ren, J. Hao, H. Feng, H. Fan, D. Zheng, D.-W. Wang, H. Wang, and S.-Y. Zhu, Generation of multicomponent atomic Schrödinger cat states of up to 20 qubits, *Science* **365**, 574 (2019).
- [4] I. M. Georgescu, S. Ashhab, and F. Nori, Quantum simulation, *Rev. Mod. Phys.* **86**, 153 (2014).
- [5] C. L. Degen, F. Reinhard, and P. Cappellaro, Quantum sensing, *Rev. Mod. Phys.* **89**, 035002 (2017).
- [6] C. J. Myatt, B. E. King, Q. A. Turchette, C. A. Sackett, D. Kielpinski, W. M. Itano, C. Monroe, and D. J. Wineland, Decoherence of quantum superpositions through coupling to engineered reservoirs, *Nature (London)* **403**, 269 (2000).
- [7] B.-H. Liu, L. Li, Y.-F. Huang, C.-F. Li, G.-C. Guo, E.-M. Laine, H.-P. Breuer, and J. Piilo, Experimental control of the transition from Markovian to non-Markovian dynamics of open quantum systems, *Nat. Phys.* **7**, 931 (2011).
- [8] M. Gessner, M. Ramm, T. Pruttivarasin, A. Buchleitner, H.-P. Breuer, and H. Häffner, Local detection of quantum correlations with a single trapped ion, *Nat. Phys.* **10**, 105 (2014).
- [9] J. F. Haase, P. J. Vetter, T. Uden, A. Smirne, J. Rosskopf, B. Naydenov, A. Stacey, F. Jelezko, M. B. Plenio, and S. F. Huelga, Controllable Non-Markovianity for a Spin Qubit in Diamond, *Phys. Rev. Lett.* **121**, 060401 (2018).
- [10] G. Andersson, B. Suri, L. Guo, T. Aref, and P. Delsing, Non-exponential decay of a giant artificial atom, *Nat. Phys.* **15**, 1123 (2019).

- [11] K.-D. Wu, Z. Hou, G.-Y. Xiang, C.-F. Li, G.-C. Guo, D. Dong, and F. Nori, Detecting non-Markovianity via quantified coherence: Theory and experiments, *arXiv:1903.03359* [npj Quantum Inf. (to be published)].
- [12] H.-P. Breuer, E.-M. Laine, J. Piilo, and B. Vacchini, Colloquium: Non-Markovian dynamics in open quantum systems, *Rev. Mod. Phys.* **88**, 021002 (2016).
- [13] H.-P. Breuer and F. Petruccione, *The Theory of Open Quantum Systems* (Oxford University Press, New York, 2007).
- [14] W.-M. Zhang, P.-Y. Lo, H.-N. Xiong, M. Wei-Yuan Tu, and F. Nori, General Non-Markovian Dynamics of Open Quantum Systems, *Phys. Rev. Lett.* **109**, 170402 (2012).
- [15] I. de Vega and D. Alonso, Dynamics of non-Markovian open quantum systems, *Rev. Mod. Phys.* **89**, 015001 (2017).
- [16] V. Giovannetti, S. Lloyd, and L. Maccone, Advances in quantum metrology, *Nat. Photonics* **5**, 222 (2011).
- [17] L. Pezzè, A. Smerzi, M. K. Oberthaler, R. Schmied, and P. Treutlein, Quantum metrology with nonclassical states of atomic ensembles, *Rev. Mod. Phys.* **90**, 035005 (2018).
- [18] A. W. Chin, S. F. Huelga, and M. B. Plenio, Quantum Metrology in Non-Markovian Environments, *Phys. Rev. Lett.* **109**, 233601 (2012).
- [19] S. L. Braunstein and C. M. Caves, Statistical Distance and the Geometry of Quantum States, *Phys. Rev. Lett.* **72**, 3439 (1994).
- [20] J. Ma, X. G. Wang, C. P. Sun, and F. Nori, Quantum spin squeezing, *Phys. Rep.* **509**, 89 (2011).
- [21] X. M. Lu, X. G. Wang, and C. P. Sun, Quantum Fisher information flow and non-Markovian processes of open systems, *Phys. Rev. A* **82**, 042103 (2010).
- [22] Á. Rivas, S. F. Huelga, and M. B. Plenio, Entanglement and Non-Markovianity of Quantum Evolutions, *Phys. Rev. Lett.* **105**, 050403 (2010).
- [23] F. Wang, P.-Y. Hou, Y.-Y. Huang, W.-G. Zhang, X.-L. Ouyang, X. Wang, X.-Z. Huang, H.-L. Zhang, L. He, X.-Y. Chang, and L.-M. Duan, Observation of entanglement sudden death and rebirth by controlling a solid-state spin bath, *Phys. Rev. B* **98**, 064306 (2018).
- [24] S. J. Peng, X. K. Xu, K. B. Xu, P. Huang, P. F. Wang, X. Kong, X. Rong, F. Z. Shi, C. K. Duan, and J. F. Du, Observation of non-Markovianity at room temperature by prolonging entanglement in solids, *Sci. Bull.* **63**, 336 (2018).
- [25] H.-P. Breuer, E.-M. Laine, and J. Piilo, Measure for the Degree of Non-Markovian Behavior of Quantum Processes in Open Systems, *Phys. Rev. Lett.* **103**, 210401 (2009).
- [26] S.-L. Chen, N. Lambert, C.-M. Li, A. Miranowicz, Y.-N. Chen, and F. Nori, Quantifying Non-Markovianity with Temporal Steering, *Phys. Rev. Lett.* **116**, 020503 (2016).
- [27] See Supplemental Material at <http://link.aps.org/supplemental/10.1103/PhysRevLett.124.210502> for the details about theoretical derivation and experimental additional data, which includes Refs. [28–38].
- [28] G. Tóth, Multipartite entanglement and high-precision metrology, *Phys. Rev. A* **85**, 022322 (2012).
- [29] L. Pezzè and A. Smerzi, Entanglement, Nonlinear Dynamics, and the Heisenberg Limit, *Phys. Rev. Lett.* **102**, 100401 (2009).
- [30] Y.-R. Zhang, Y. Zeng, H. Fan, J. Q. You, and F. Nori, Characterization of Topological States Via Dual Multipartite Entanglement, *Phys. Rev. Lett.* **120**, 250501 (2018).
- [31] Á. Rivas, S. F. Huelga, and M. B. Plenio, Quantum non-Markovianity: Characterization, quantification and detection, *Rep. Prog. Phys.* **77**, 094001 (2014).
- [32] L. Marseglia, J. P. Hadden, A. C. Stanley-Clarke, J. P. Harrison, B. Patton, Y.-L. D. Ho, B. Naydenov, F. Jelezko, J. Meijer, P. R. Dolan, J. M. Smith, J. G. Rarity, and J. L. O'Brien, Nanofabricated solid immersion lenses registered to single emitters in diamond, *Appl. Phys. Lett.* **98**, 133107 (2011).
- [33] B. Smeltzer, L. Childress, and A. Gali,  $^{13}\text{C}$  hyperfine interactions in the nitrogen-vacancy centre in diamond, *New J. Phys.* **13**, 025021 (2011).
- [34] A. Dréau, J.-R. Maze, M. Lesik, J.-F. Roch, and V. Jacques, High-resolution spectroscopy of single NV defects coupled with nearby  $^{13}\text{C}$  nuclear spins in diamond, *Phys. Rev. B* **85**, 134107 (2012).
- [35] A. Jarmola, V. M. Acosta, K. Jensen, S. Chemerisov, and D. Budker, Temperature- and Magnetic-Field-Dependent Longitudinal Spin Relaxation in Nitrogen-Vacancy Ensembles in Diamond, *Phys. Rev. Lett.* **108**, 197601 (2012).
- [36] P. C. Maurer, G. Kucsko, C. Latta, L. Jiang, N. Y. Yao, S. D. Bennett, F. Pastawski, D. Hunger, N. Chisholm, M. Markham, D. J. Twitchen, J. I. Cirac, and M. D. Lukin, Room-temperature quantum bit memory exceeding one second, *Science* **336**, 1283 (2012).
- [37] T. van der Sar, Z. H. Wang, M. S. Blok, H. Bernien, T. H. Taminiou, D. M. Toyli, D. A. Lidar, D. D. Awschalom, R. Hanson, and V. V. Dobrovitski, Decoherence-protected quantum gates for a hybrid solid-state spin register, *Nature (London)* **484**, 82 (2012).
- [38] G.-Q. Liu, H. C. Po, J.-F. Du, R.-B. Liu, and X.-Y. Pan, Noise-resilient quantum evolution steered by dynamical decoupling, *Nat. Commun.* **4**, 2254 (2013).
- [39] M. W. Doherty, N. B. Manson, P. Delaney, F. Jelezko, J. Wrachtrup, and L. C. L. Hollenberg, The nitrogen-vacancy colour centre in diamond, *Phys. Rep.* **528**, 1 (2013).
- [40] V. Jacques, P. Neumann, J. Beck, M. Markham, D. Twitchen, J. Meijer, F. Kaiser, G. Balasubramanian, F. Jelezko, and J. Wrachtrup, Dynamic Polarization of Single Nuclear Spins by Optical Pumping of Nitrogen-Vacancy Color Centers in Diamond at Room Temperature, *Phys. Rev. Lett.* **102**, 057403 (2009).
- [41] L. Childress, M. V. Gurudev Dutt, J. M. Taylor, A. S. Zibrov, F. Jelezko, J. Wrachtrup, P. R. Hemmer, and M. D. Lukin, Coherent dynamics of coupled electron and nuclear spin qubits in diamond, *Science* **314**, 281 (2006).
- [42] G.-Q. Liu, Y.-R. Zhang, Y.-C. Chang, J.-D. Yue, H. Fan, and X.-Y. Pan, Demonstration of entanglement-enhanced phase estimation in solid, *Nat. Commun.* **6**, 6726 (2015).
- [43] Z.-P. Liu, J. Zhang, Ş. K. Özdemir, B. Peng, H. Jing, X.-Y. Lü, C.-W. Li, L. Yang, F. Nori, and Y.-X. Liu, Metrology with  $\mathcal{PT}$ -Symmetric Cavities: Enhanced Sensitivity Near the  $\mathcal{PT}$ -Phase Transition, *Phys. Rev. Lett.* **117**, 110802 (2016).
- [44] S. F. Huelga, Á. Rivas, and M. B. Plenio, Non-Markovianity-Assisted Steady State Entanglement, *Phys. Rev. Lett.* **108**, 160402 (2012).

- [45] S. Gröblacher, A. Trubarov, N. Prigge, G.D. Cole, M. Aspelmeyer, and J. Eisert, Observation of non-Markovian micromechanical Brownian motion, *Nat. Commun.* **6**, 7606 (2015).
- [46] C.-F. Li, G.-C. Guo, and J. Piilo, Non-Markovian quantum dynamics: What is it good for?, *Europhys. Lett.* **128**, 30001 (2020).
- [47] Y. Dong, Y. Zheng, S. Li, C.-C. Li, X.-D. Chen, G.-C. Guo, and F.-W. Sun, Non-Markovianity-assisted high-fidelity Deutsch-Jozsa algorithm in diamond, *Quantum Inf.* **4**, 3 (2018).
- [48] B.-H. Liu, X.-M. Hu, Y.-F. Huang, C.-F. Li, G.-C. Guo, A. Karlsson, E.-M. Laine, S. Maniscalco, C. Macchiavello, and J. Piilo, Efficient superdense coding in the presence of non-Markovian noise, *Europhys. Lett.* **114**, 10005 (2016).
- [49] N. Zhao, Z.-Y. Wang, and R.-B. Liu, Anomalous Decoherence Effect in a Quantum Bath, *Phys. Rev. Lett.* **106**, 217205 (2011).
- [50] P. Huang, X. Kong, N. Zhao, F. Z. Shi, P. F. Wang, X. Rong, R.-B. Liu, and J.F. Du, Observation of an anomalous decoherence effect in a quantum bath at room temperature, *Nat. Commun.* **2**, 570 (2011).
- [51] L. B. Ho, Y. Matsuzaki, M. Matsuzaki, and Y. Kondo, Realization of controllable open system with NMR, *New J. Phys.* **21**, 093008 (2019).
- [52] Z.-L. Xiang, S. Ashhab, J. Q. You, and F. Nori, Hybrid quantum circuits: Superconducting circuits interacting with other quantum systems, *Rev. Mod. Phys.* **85**, 623 (2013).